

Thermalization and its mechanism for generic isolated quantum systems

Marcos Rigol,^{1,2} Vanja Dunjko,^{1,2} and Maxim Olshanii²

¹*Department of Physics & Astronomy, University of Southern California, Los Angeles, CA 90089, USA*

²*Department of Physics, University of Massachusetts Boston, Boston, MA 02125, USA*

Time dynamics of isolated many-body quantum systems has long been an elusive subject, perhaps most urgently needed in the foundations of quantum statistical mechanics. Only very recently experimentalists have begun performing detailed studies of this matter [1, 2]. In generic systems, one expects the nonequilibrium dynamics to lead to thermalization [3]: a relaxation to states where the values of macroscopic quantities are stationary, universal with respect to widely differing initial conditions, and predictable through the time-tested recipe of statistical mechanics. The relaxation mechanism is not obvious, however; for example, dynamical chaos cannot play the key role as it does in classical systems [4] since quantum evolution is linear. That new rules could apply to isolated quantum systems was underscored by recent studies suggesting that statistical mechanics may give wrong predictions for their relaxation [5, 6]. Here we demonstrate that a generic quantum many-body system does relax to a state well-described by standard statistical mechanical prescription. Moreover, we show that time evolution itself plays a merely auxiliary role and that thermalization happens instead at the level of individual eigenstates, as first proposed by M. Srednicki [7]. Due to this *eigenstate thermalization* scenario, thermalization joins the list of processes that, like scattering, seem intrinsically temporal, and yet in quantum mechanics effectively become time-independent problems.

If we pierce an inflated balloon inside a vacuum chamber, very soon we find the released air uniformly filling the enclosure and the air molecules attaining the Maxwell velocity distribution whose width depends only on their total number and energy. Different balloon shapes, placements, or piercing points all lead to the same spatial and velocity distributions. Classical physics explains this *thermodynamical universality* as follows [4]: almost all particle trajectories quickly begin looking alike, even if their initial points are very different, because nonlinear equations drive them to explore ergodically the constant-energy manifold, covering it uniformly with respect to precisely the microcanonical measure. However, if the system is integrable, i.e. possesses a sufficient number of *functionally independent* conserved quantities in mutual involution, then time evolution is confined to a highly restricted hypersurface of the energy manifold. Hence, microcanonical predictions fail and the system does not thermalize.

On the other hand, in isolated quantum systems not only is dynamical chaos absent due to the linearity of time evolution, but also the straightforward link between integrability and conserved quantities no longer exists [8]. In quantum mechanics commuting operators cannot be functionally independent, but only linearly independent. However, for *any* isolated system one can always construct sets—as large as the Hilbert space!—of linearly independent mutually commuting conserved quantities: one example is the projectors $\hat{P}_\alpha = |\Psi_\alpha\rangle\langle\Psi_\alpha|$ to the eigenstates of the Hamiltonian [8]. Thus it is unclear whether thermalization should never occur—because conserved quantities are always present—or always occur—because conserved quantities are never functionally independent.

By this logic, our previous work [9, 10] would seem to suggest the former. There we showed that an integrable isolated one-dimensional system of hard-core bosons relaxes to an equilibrium characterized by a *generalized* Gibbs ensemble, in which conserved quantities play a crucial role. The

ensemble works for a wide variety of initial conditions [11] as well as for a fermionic system [12]. It also explains a recent experimental result: the absence of thermalization in the Tonks-Girardeau gas [1].

More generally, the high levels of isolation [1, 13, 14] and control [15, 16] possible in experiments with ultracold quantum gases have increased the theoretical attention to thermalization in isolated systems. However, despite numerous studies of specific models there is not yet consensus on how or even if relaxation to the usual thermal values occurs for non-integrable systems [17]. Common wisdom says that it does [3], but some recent numerical results suggest otherwise, either under certain conditions [5] or in general [6].

In order to understand the relaxation process in isolated quantum systems, we studied the time evolution of five hard-core bosons with additional weak nearest-neighbor repulsions, on a 21-site two-dimensional lattice, initially confined to a portion of the lattice and prepared in their ground state there. The relaxation dynamics begins when the confinement is lifted. Figure 1A shows the exact geometry [18]. Expanding the initial state wavefunction in the eigenstate basis of the final Hamiltonian \hat{H} as $|\psi(0)\rangle = \sum_\alpha C_\alpha |\Psi_\alpha\rangle$, the many-body wavefunction evolves as $|\psi(t)\rangle = e^{-i\hat{H}t}|\psi(0)\rangle = \sum_\alpha C_\alpha e^{-iE_\alpha t} |\Psi_\alpha\rangle$, where the E_α 's are the eigenstate energies. Thus obtaining numerically-exact results for all times required the full diagonalization of the 20 349-dimensional Hamiltonian. The quantum-mechanical mean of any observable \hat{A} evolves as

$$\langle \hat{A}(t) \rangle \equiv \langle \psi(t) | \hat{A} | \psi(t) \rangle = \sum_{\alpha', \alpha} C_{\alpha'}^* C_\alpha e^{i(E_{\alpha'} - E_\alpha)t} A_{\alpha'\alpha}, \quad (1)$$

with $A_{\alpha'\alpha} = \langle \Psi_{\alpha'} | \hat{A} | \Psi_\alpha \rangle$. The long-time average of $\langle \hat{A}(t) \rangle$ is then

$$\overline{\langle \hat{A} \rangle} = \sum_\alpha |C_\alpha|^2 A_{\alpha\alpha}. \quad (2)$$

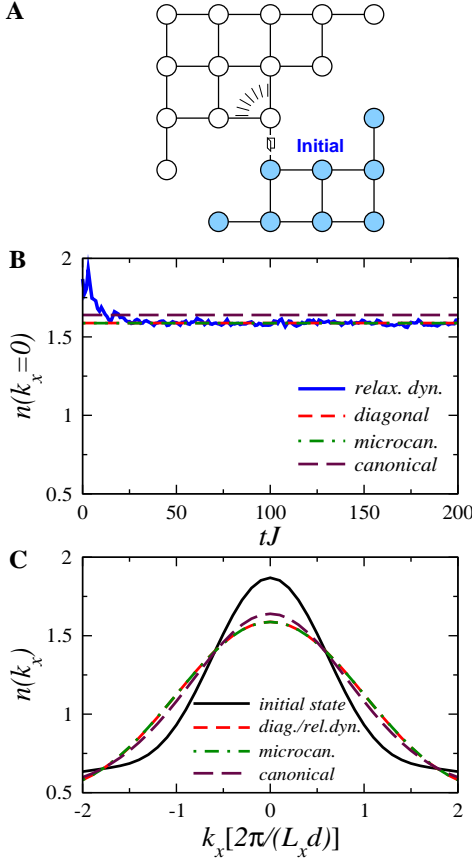


FIG. 1: (A) Two-dimensional lattice on which five hard-core bosons propagate in time. The bosons are initially prepared in the ground state of the sub-lattice in the lower-right corner and released through the indicated link. (B) The corresponding relaxation dynamics of the marginal momentum distribution center $[n(k_x = 0)]$ compared with the predictions of the three ensembles. In the microcanonical case, we averaged over all eigenstates whose energies lie within a narrow window $[E_0 - \Delta E, E_0 + \Delta E]$. Here $E_0 \equiv \langle \psi(0) | \hat{H} | \psi(0) \rangle = \langle \psi(t) | \hat{H} | \psi(t) \rangle$ is $-5.06J$, and $\Delta E = 0.1J$, where J is the hopping parameter. [Our predictions are robust with respect to this value of ΔE [18].] We set the canonical ensemble temperature to $k_B T = 1.87J$, where k_B is the Boltzmann constant, so that the ensemble prediction for the energy is E_0 . (C) Full momentum distribution function in the initial state, after relaxation, and in the different ensembles. Here d is the lattice constant and $L_x = 5$ the lattice width.

Note that if the system relaxes at all, it must be to this value. We find it convenient to think of Eq. (2) as stating the prediction of a “diagonal ensemble,” $|C_\alpha|^2$ corresponding to the weight $|\Psi_\alpha\rangle$ has in the ensemble. In fact, this ensemble is precisely the constrained ensemble of Ref. [10] if as the integrals of motion one takes all the projection operators $\hat{P}_\alpha = |\Psi_\alpha\rangle\langle\Psi_\alpha|$ [19].

Now if the quantum-mechanical mean of an observable behaves thermally it should settle to the prediction of an appropriate statistical-mechanical ensemble. For our numerical experiments we chose to monitor the marginal momentum distribution along the horizontal axis $n(k_x)$ and its central component $n(k_x = 0)$ [18]. Figures 1B and 1C demonstrate that

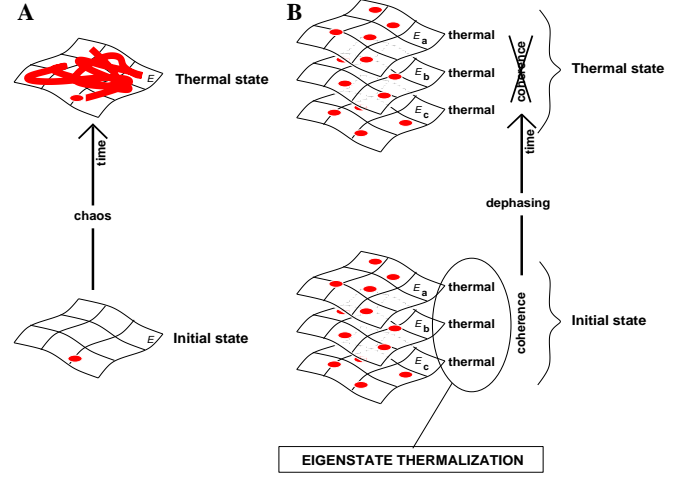


FIG. 2: (A) In classical mechanics, time evolution constructs the thermal state from an initial state that generally bears no resemblance to the former. (B) In quantum mechanics, according to the eigenstate thermalization hypothesis, every eigenstate of the Hamiltonian always implicitly contains a thermal state. The coherence between the eigenstates initially hides it, but time dynamics reveals it through dephasing.

both relax to their microcanonical predictions. The diagonal ensemble predictions are indistinct from these, but the canonical ones, although quite close, are not—an indication of the relevance of finite size effects, which may be the origin of some of the apparent deviations from thermodynamics in recent numerical studies [5, 6].

Having established that the microcanonical ensemble gives the correct predictions, we can now pinpoint why this success is very puzzling. We seem to have found an observable \hat{A} — the momentum distribution—that satisfies $\sum_\alpha |C_\alpha|^2 A_{\alpha\alpha} = \langle A \rangle_{\text{microcan.}}(E_0)$, where the right-hand side is the microcanonical prediction with the energy window centered at E_0 . But this seems impossible, since the left hand side depends on the details of the initial conditions through the coefficients $C_\alpha = \langle \Psi_\alpha | \psi(0) \rangle$, while the right hand side depends only on the initial energy.

In 1994, Srednicki [7] realized that since one expects the $|C_\alpha|^2$ values to be narrowly peaked around the mean energy, the paradox disappears if the eigenstate expectation values $A_{\alpha\alpha} = \langle \Psi_\alpha | \hat{A} | \Psi_\alpha \rangle$ are all approximately the same for eigenstates $|\Psi_\alpha\rangle$ whose energies lie within the microcanonical window. In other words, he used the paradox to motivate the

Eigenstate thermalization hypothesis (ETH) [Srednicki (1994) [7]].

The expectation value $\langle \Psi_\alpha | \hat{A} | \Psi_\alpha \rangle$ of a few-body observable \hat{A} in an eigenstate of the Hamiltonian $|\Psi_\alpha\rangle$, with energy E_α , of a large interacting many-body system equals the thermal (microcanonical in our case) average $\langle A \rangle_{\text{microcan.}}(E_\alpha)$ of \hat{A} at the mean energy E_α :

$$\langle \Psi_\alpha | \hat{A} | \Psi_\alpha \rangle = \langle A \rangle_{\text{microcan.}}(E_\alpha). \quad (3)$$

The ETH suggests that classical and quantum thermal states

have very different natures, as depicted in Fig. 2. While at present there are no general theoretical arguments supporting the ETH, some results exist for restricted classes of systems. To begin with, there are rigorous proofs that some particular quantum systems, whose classical counterparts are chaotic, satisfy the ETH in the semiclassical limit [20, 21, 22, 23]. More generally, for low density billiards in the semiclassical regime the ETH follows from Berry's conjecture [7], which

in turn is believed to hold in semiclassical classically-chaotic systems [24]. At the other end of the chaos-integrability continuum, in systems solvable by Bethe ansatz, observables are smooth functions of the integrals of motion, which allows the construction of single states that reproduce thermal predictions [25]. Finally, there is a rigorous proof that the ETH is valid for internal observables of a system weakly coupled to a large reservoir [26].

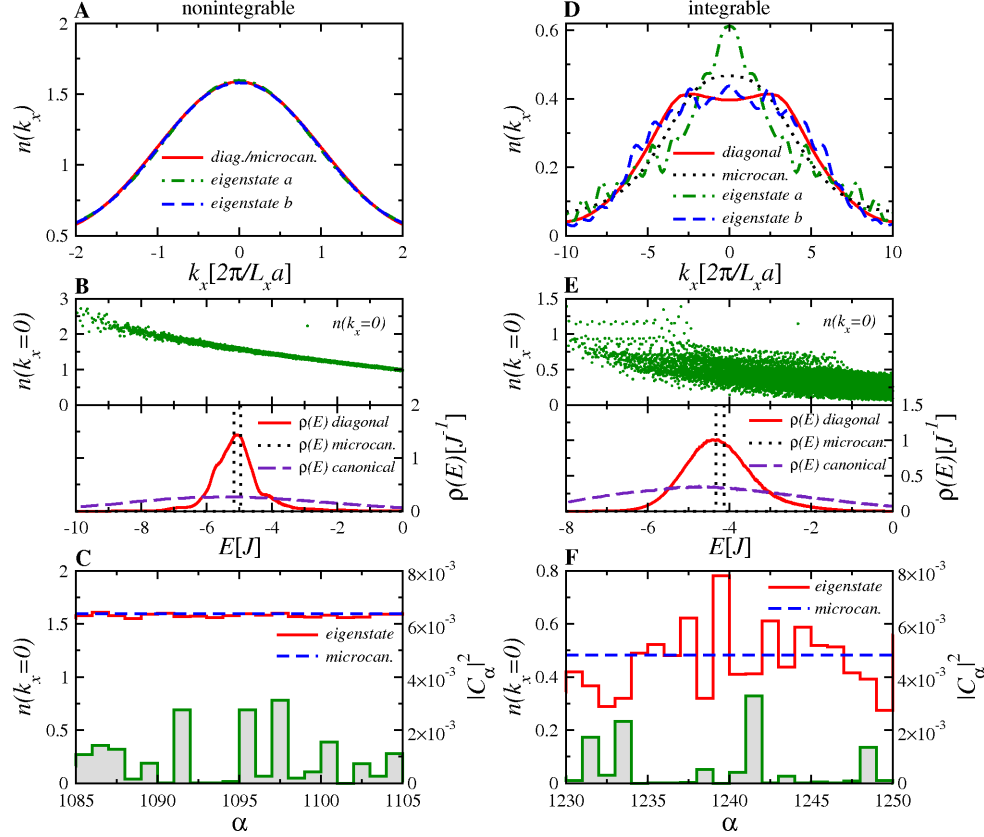


FIG. 3: (A) In our nonintegrable system, the momentum distribution $n(k_x)$ for two typical eigenstates with energies close to E_0 is identical to the microcanonical result, in accordance with the ETH. (B) Upper panel: $n(k_x = 0)$ eigenstate expectation value (EEV) as a function of the eigenstate energy resemble a smooth curve. Lower panel: the energy distribution $\rho(E)$ of the three ensembles considered in this work. (C) Detailed view of $n(k_x = 0)$ (left labels) and $|C_\alpha|^2$ (right labels) for 20 eigenstates around E_0 . (D) In the integrable system, $n(k_x)$ for two eigenstates with energies close to E_0 and for the microcanonical and diagonal ensembles are very different from each other, i.e., the ETH fails. (E) Upper panel: $n(k_x = 0)$ EEV considered as a function of the eigenstate energy gives a thick cloud of points rather than resembling a smooth curve. Lower panel: energy distributions in the integrable system are similar to the nonintegrable ones depicted in B. (F) Correlation between $n(k_x = 0)$ and $|C_\alpha|^2$ for 20 eigenstates around E_0 . It explains why in D the microcanonical prediction for $n(k_x = 0)$ is larger than the diagonal one.

In Figs. 3A-C we demonstrate that ETH is the mechanism responsible for thermal behavior in our nonintegrable system. Thermal behavior also requires that both the diagonal and the chosen thermal ensemble have energy distributions $\rho(E)$ [= probability distribution \times the density of states] that are sufficiently narrow so that in the energy region where $\rho(E)$ is appreciable, the derivative of the curve EEV vs the energy does not change much [18]. As shown in Fig. 3B, this holds for the microcanonical and diagonal ensembles but not for the canonical ensemble, explaining the failure of the latter to describe relaxation in Fig. 1.

On the other hand, figures 3D-F show how the ETH *fails* for an isolated one-dimensional *integrable* system. The latter consists of five hard-core bosons initially prepared in their ground state in an 8-site chain, one of the ends of which we then link to one of the ends of an adjoining (empty) 13-site chain to trigger relaxation dynamics. As Fig. 3E shows, $n(k_x)$ as a function of energy is a broad cloud of points, meaning that the ETH is not valid.

Nevertheless, one may still wonder if the averages over the diagonal and the microcanonical energy distributions shown in Fig. 3E might agree. Figure 3D shows that this does not

happen. This is so because, as shown in Fig. 3F, the values of $n(k_x = 0)$ for the most-occupied states in the diagonal ensemble (the largest values of $|C_\alpha|^2$) are always smaller than the microcanonical prediction, and those of the least-occupied states, always larger. Hence, correlations between the values of $n(k_x = 0)$ and $|C_\alpha|^2$ preclude thermalization. These correlations have their origin in the nontrivial integrals of motion that make the system integrable and that enter the *generalized* Gibbs ensemble, introduced in Ref. [10], as appropriate for formulating statistical mechanics of isolated integrable systems. In the nonintegrable case shown in Fig. 3C, $n(k_x = 0)$ is so narrowly distributed that it does not matter whether or not it is correlated with $|C_\alpha|^2$ [28].

The thermalization mechanism outlined thus far explains why long-time averages converge to their thermal predictions. A striking aspect of Fig. 1B, however, is that the time fluctuations are so small that after relaxation the thermal prediction works well at every instant of time. Looking at Eq. (1), one might think this is so because the contribution of the off-diagonal terms gets attenuated by temporal dephasing, which results from the generic incommensurability of the frequencies of the oscillating exponentials. However, this attenuation only scales as the root of the number of dephasing terms, and is exactly compensated by their larger number: if the number of eigenstates that have a significant overlap with the initial state is N_{states} , then typical $C_\alpha \sim 1/\sqrt{N_{\text{states}}}$, and the sum over off-diagonal terms in Eq. (1) finally does not scale down with N_{states} :

$$\sum_{\substack{\alpha', \alpha \\ \alpha' \neq \alpha}} \frac{e^{i(E_{\alpha'} - E_\alpha)t}}{N_{\text{states}}} A_{\alpha'\alpha} \sim \frac{\sqrt{N_{\text{states}}^2}}{N_{\text{states}}} A_{\alpha'\alpha}^{\text{typical}} \sim A_{\alpha'\alpha}^{\text{typical}} \quad (4)$$

Hence, were the magnitude of the diagonal and off-diagonal terms comparable, their contributions would be comparable as well, and time fluctuations of the average would be of the order of the average. However, this is not the case and thus

$$A_{\alpha'\alpha}^{\text{typical}} \ll A_{\alpha\alpha}^{\text{typical}}. \quad (5)$$

Figure 4A confirms this inequality for the matrix elements of the momentum distribution in our system. We should mention that there is an *a priori* argument—admittedly in part dependent on certain hypotheses about chaos in quantum billiards—in support of this inequality for the case when the mean value of \hat{A} in an energy eigenstate is comparable to the quantum fluctuation of \hat{A} in that state [29].

On the other hand, the thermalization we see appears to be working a bit *too well*: one would expect the fluctuations measured in an experimental system as small as ours to be much larger than what Fig. 1B shows. Figure 4B presents the resolution of this final puzzle. The fluctuations that one would actually measure would be dominated by the quantum fluctuations of the time-dependent state. The rather large size of the quantum fluctuations relative to the thermal mean value is of course particular to small systems; however, the dominance of the quantum fluctuations over the temporal fluctuations of

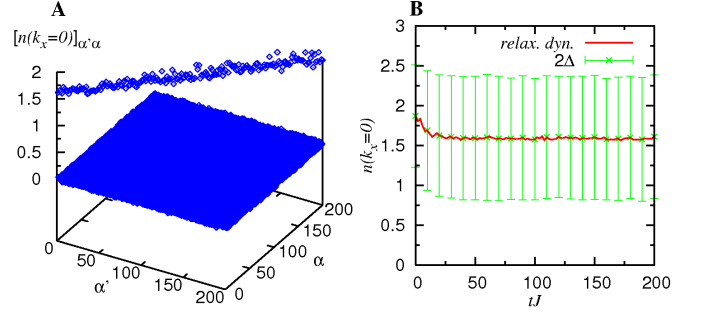


FIG. 4: (A) Matrix elements of the observable of interest, $n(k_x = 0)$, as a function of state indices; the eigenstates of the Hamiltonian are indexed in the order of diminishing overlap with the initial state. The dominance of the diagonal matrix elements is apparent. (B) The same time evolution as in Figure 1B with the error bars showing the quantum fluctuations $n(k_x = 0) \pm \Delta$ with $\Delta = [\langle \hat{n}^2(k_x = 0) \rangle - \langle \hat{n}(k_x = 0) \rangle^2]^{1/2}$, which are clearly much larger than the temporal fluctuations of $n(k_x = 0)$.

quantum expectation values is not and is actually expected for generic systems in the thermodynamic limit [27].

We have demonstrated that, in contrast to the integrable case, the nonequilibrium dynamics of a generic isolated quantum system does lead to standard thermalization. Our verification that this happens through the eigenstate thermalization mechanism, which M. Srednicki compellingly defended for the case of rarefied semiclassical quantum billiards but conjectured to be valid in general, strongly suggests that quantum relaxation indeed generally follows this scenario. The role of time in quantum thermalization is then merely to lift a veil hiding the intrinsically thermal nature of individual energy eigenstates. This general property of eigenstates may serve as a key input in future research on the structure of many-body Hamiltonians.

This work was supported by the US National Science Foundation Grant No. PHY-0301052 and the Office of Naval Research Grant No. N00014-03-1-0427. We are grateful to the USC HPC center where all our computations have been performed. We thank A. C. Cassidy, K. Jacobs, and A. P. Young for helpful comments.

METHODS

The Hamiltonian and the numerical calculations

In a system of units where $\hbar = 1$ the Hamiltonian reads

$$\hat{H} = -J \sum_{\langle i,j \rangle} (\hat{b}_i^\dagger \hat{b}_j + \text{h.c.}) + U \sum_{\langle i,j \rangle} \hat{n}_i \hat{n}_j \quad (6)$$

where $\langle i, j \rangle$ indicates that the sums run over all nearest-neighbor pairs of sites, J is the hopping parameter, and U the nearest-neighbor repulsion parameter that we always set

to $0.1J$. The hard-core boson creation (\hat{b}_i^\dagger) and annihilation (\hat{b}_j) operators commute on different sites, $[\hat{b}_i, \hat{b}_j^\dagger] = [\hat{b}_i, \hat{b}_j] = [\hat{b}_i^\dagger, \hat{b}_j^\dagger] = 0$ for all i and $j \neq i$, while the hard-core condition imposes the canonical anticommutation relations on the same site, $\{\hat{b}_i, \hat{b}_i^\dagger\} = 1$, and $(\hat{b}_i)^2 = (\hat{b}_i^\dagger)^2 = 0$ for all i . Here $\hat{n}_i = \hat{b}_i^\dagger \hat{b}_i$ is the density operator.

An exact study of the nonequilibrium dynamics for *all* time scales requires a full diagonalization of the many-body Hamiltonian (6). We are able to fully diagonalize matrices of dimension $D \sim 20\,000$, and so we consider $N = 5$ hard-core bosons on a 5×5 lattice with four sites missing ($D = 20\,349$); see Fig. 5. All the eigenstates of the Hamiltonian are used for the time evolution

$$|\psi(t)\rangle = \exp[-i\hat{H}t]|\psi(0)\rangle = \sum_{\alpha} C_{\alpha} \exp[-iE_{\alpha}t]|\Psi_{\alpha}\rangle,$$

where $|\psi(t)\rangle$ is the time-evolving state, $|\psi(0)\rangle$ the initial state, $|\Psi_{\alpha}\rangle$ the eigenstates of the Hamiltonian with the energies E_{α} , and $C_{\alpha} = \langle\Psi_{\alpha}|\psi(0)\rangle$. Our initial state is the ground state of the five bosons when they are confined to the lower part of the lattice (the colored part in Fig. 5). The time evolution begins with the opening of the link shown in Fig. 5, which allows the bosons to expand over the whole lattice. The position of the missing sites was chosen so that we only open a single link to start the relaxation dynamics. The motivation for this will become apparent in the last paragraph below.

As the principal observables of interest we chose the marginal momentum distribution along the horizontal axis $n(k_x) = \sum_{k_y} n(k_x, k_y)$ and in particular its central component $n(k_x = 0)$, quantities readily measurable in actual experiments with ultracold quantum gases [15]. Here the full two-dimensional momentum distribution is $n(k_x, k_y) = 1/L^2 \sum_{i,j} e^{-i2\pi\mathbf{k}(\mathbf{r}_i - \mathbf{r}_j)/L} \langle\hat{b}_i^\dagger \hat{b}_j\rangle$, where $L = L_x = L_y = 5$ are the linear sizes of the lattice. The position $\mathbf{r}_i = (i_x d, i_y d)$ involves the lattice constant d .

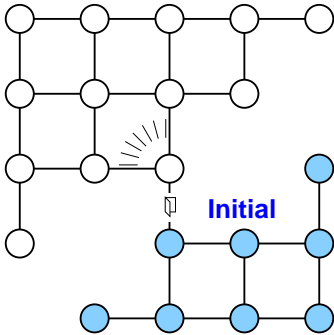


FIG. 5: Two-dimensional lattice on which the particles propagate in time. The initial state is the ground state of 5 hard-core bosons confined to the sub-lattice in the lower right-hand corner, and the time evolution starts after the opening of the link indicated by the door symbol.

The microcanonical ensemble in a small system

To compute the microcanonical ensemble predictions, we have averaged over all eigenstates whose energies lie within a narrow window $[E_0 - \Delta E, E_0 + \Delta E]$, with $E_0 \equiv \langle\psi(0)|\hat{H}|\psi(0)\rangle = -5.06J$. Since our systems are small there is generally no meaning to the limit $\Delta E \rightarrow 0$, because small enough windows may fail to contain even a single eigenstate. Instead, one should show that the microcanonical predictions are robust with respect to the choice of the width of the energy window. In Fig. 6 we demonstrate this robustness in a neighborhood of $\Delta E = 0.1J$, a value that seems to be an appropriate choice given the data presented in the inset of the same figure. There we show the dependence on ΔE of the predictions for $n(k_x = 0)$ given by the “left-averaged” and the “right-averaged” microcanonical ensembles, by which we mean that the microcanonical windows are chosen as $[E_0 - \Delta E, E_0]$ and $[E_0, E_0 + \Delta E]$, respectively. We see that for $\Delta E \lesssim 0.1J$, the two microcanonical predictions are almost independent of the value of ΔE . The main panel in Fig. 6 shows that the microcanonical values of $n(k_x)$ for $\Delta E = 0.05J$ and for $\Delta E = 0.1J$ are indistinguishable.

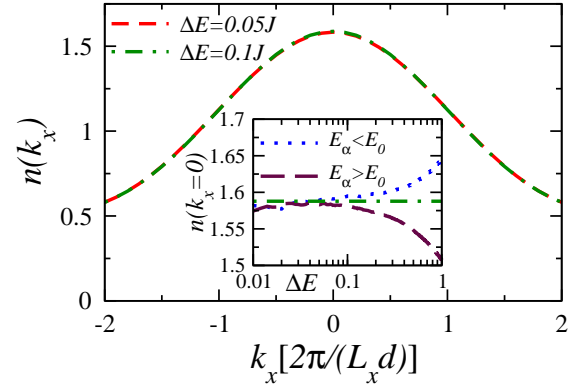


FIG. 6: Microcanonical momentum distribution function for two different values of ΔE . Inset: Microcanonical predictions for $n(k_x = 0)$ calculated using the left ($[E_0 - \Delta E, E_0]$) and the right ($[E_0, E_0 + \Delta E]$) averages as functions of ΔE .

Eigenstate thermalization and the width of the energy distribution

The eigenstate thermalization alone is not sufficient to ensure an agreement between the predictions of the diagonal and thermal ensembles. As discussed in [7], it is also necessary that both distributions be sufficiently narrow. More specifically, one must require for both ensembles

$$(\Delta E)^2 |A''(E)/A(E)| \ll 1, \quad (7)$$

where ΔE is the width of the energy distribution in the ensemble, and $A(E)$ is the dependence of the expectation value

of the observable $A_{\alpha\alpha} = \langle \Psi_\alpha | \hat{A} | \Psi_\alpha \rangle$ on the energy E_α of the Hamiltonian-operator eigenstate $|\Psi_\alpha\rangle$. Note that because of eigenstate thermalization, $A(E)$ is a smooth function of energy. For the thermodynamical ensembles the condition (7) is always satisfied in the thermodynamic limit. We now show that it is also satisfied for the diagonal ensemble in the thermodynamic limit.

If one considers an observable a that is the intensive counterpart of A , all conclusions obtained for a can be extended to the original observable A via trivial rescaling. For example, for our principal observable of interest, $n(k_x)$, the corresponding intensive variable is the momentum density $\xi(p_x)$ normalized as $\int dp_x \xi(p_x) = 1$. Notice that in this case $\xi(p_x) = n(k_x)L_x d/(2\pi N)$.

For a , the condition in (7) reduces to

$$(\Delta\epsilon)^2 |a''(\epsilon)/a(\epsilon)| \ll 1, \quad (8)$$

where $\epsilon \equiv E/N$. For sufficiently large systems the dependence of a on ϵ is independent of the system size. Hence, in order to justify the validity of (8) it is sufficient to prove that the width of the distribution of the energy per particle in the diagonal ensemble converges to zero for large linear sizes L of the system:

$$\Delta\epsilon \xrightarrow{L \rightarrow \infty} 0. \quad (9)$$

Suppose that initially our system is prepared in an eigenstate $|\Psi_0\rangle$ of a Hamiltonian \hat{H}_0 and that at time $t = 0$ the Hamiltonian is suddenly changed to \hat{H} :

$$\hat{H}_0 \rightarrow \hat{H} = \hat{H}_0 + \hat{W},$$

where \hat{W} is the difference between the new and the old Hamiltonians. Within this scenario, the energy width

$$\Delta E = \sqrt{\sum_\alpha E_\alpha^2 |C_\alpha|^2 - \left(\sum_\alpha E_\alpha |C_\alpha|^2 \right)^2}$$

of the diagonal ensemble becomes equal to the variance of the new energy in the state $|\Psi_0\rangle$:

$$\Delta E = \Delta H \equiv \sqrt{\langle \Psi_0 | \hat{H}^2 | \Psi_0 \rangle - \langle \Psi_0 | \hat{H} | \Psi_0 \rangle^2}.$$

It is now straightforward to show that the variance of \hat{H} equals the variance of \hat{W} :

$$\Delta H = \Delta W.$$

In order to deduce how ΔW scales in the thermodynamic limit, we assume that \hat{W} is a sum of local operators $\hat{w}(j)$ over some region of the lattice σ (a single point, a straight line, the whole lattice, etc.):

$$\hat{W} = \sum_{j \in \sigma} \hat{w}(j).$$

Here $\hat{w}(j)$ is a polynomial of creation and annihilation operators localized at the points $j + \Delta j$, where $|\Delta j|$ is limited from the above by a finite number that does not scale with the system size. The mean square of \hat{W} can be written as

$$\begin{aligned} \langle \Psi_0 | \hat{W}^2 | \Psi_0 \rangle &= \langle \Psi_0 | \hat{W} | \Psi_0 \rangle^2 \\ &+ \sum_{j_1, j_2 \in \sigma} [\langle \Psi_0 | \hat{w}(j_1) \hat{w}(j_2) | \Psi_0 \rangle \\ &- \langle \Psi_0 | \hat{w}(j_1) | \Psi_0 \rangle \langle \Psi_0 | \hat{w}(j_2) | \Psi_0 \rangle]. \end{aligned} \quad (10)$$

In the absence of long-range correlations the expression in brackets tends to zero for large distances between j_1 and j_2 . Therefore, the whole second term on the right-hand-side of (10) scales as L^{d_σ} , where d_σ is the dimensionality of the sublattice σ and L is the linear size of the lattice. The variance of \hat{W} scales the same way:

$$(\Delta W)^2 \xrightarrow{L \rightarrow \infty} L^{d_\sigma}.$$

Retracing our steps, we arrive at the conclusion that the energy width $\Delta\epsilon$ indeed tends to zero in the thermodynamic limit:

$$\Delta\epsilon \xrightarrow{L \rightarrow \infty} \frac{1}{L^{d_L - d_\sigma/2}},$$

where $d_L \geq d_\sigma$ is the dimensionality of the whole lattice.

Note that for the two-dimensional lattice considered in this paper the role of \hat{W} is played by the hopping energy of the “door” link. An analysis similar to the one above shows that increasing the number of “door” links will lead to an increase in the width $\Delta\epsilon$, proportional to the square root of the number of “door” links. This is why in our 2D experiment, we have chosen the position of the missing sites to be the one in Fig. 5, so that only a single link is opened during the time evolution.

-
- [1] Kinoshita, T., Wenger, T. & Weiss, D. S. A quantum Newton’s cradle. *Nature (London)* **440**, 900 (2006).
 - [2] Hofferberth, S., Lesanovsky, I., Fischer, B., Schumm, T. & Schmiedmayer, J. Non-equilibrium coherence dynamics in one-dimensional bose gases. arXiv:0706.2259, to appear in *Nature*.
 - [3] Sengupta, K., Powell, S. & Sachdev, S. Quench dynamics across quantum critical points. *Phys. Rev. A* **69**, 053616 (2004).
 - [4] Gallavotti, G. *Statistical Mechanics: A Short Treatise* (Springer, Berlin, 1999).
 - [5] Kollath, C., Läuchli, A. & Altman, E. Quench dynamics and nonequilibrium phase diagram of the Bose-Hubbard model. *Phys. Rev. Lett.* **98**, 180601 (2007).
 - [6] Manmana, S. R., Wessel, S., Noack, R. M. & Muramatsu, A. Strongly correlated fermions after a quantum quench. *Phys. Rev. Lett.* **98**, 210405 (2007).
 - [7] Srednicki, M. Chaos and quantum thermalization. *Phys. Rev. E* **50**, 888 (1994).
 - [8] Sutherland, B. *Beautiful Models* (World Scientific, Singapore, 2004).
 - [9] With V. Yurovsky.

- [10] Rigol, M., Dunjko, V., Yurovsky, V. & Olshanii, M. Relaxation in a completely integrable many-body quantum system: An ab initio study of the dynamics of the highly excited states of 1D lattice hard-core bosons. *Phys. Rev. Lett.* **98**, 050405 (2007).
- [11] Rigol, M., Muramatsu, A. & Olshanii, M. Hard-core bosons on optical superlattices: Dynamics and relaxation in the superfluid and insulating regimes. *Phys. Rev. A* **74**, 053616 (2006).
- [12] Cazalilla, M. A. Effect of suddenly turning on interactions in the Luttinger model. *Phys. Rev. Lett.* **97**, 156403 (2006).
- [13] Jin, D. S., Ensher, J. R., Matthews, M. R., Wieman, C. E. & Cornell, E. A. Collective excitations of a Bose-Einstein condensate in a dilute gas. *Phys. Rev. Lett.* **77**, 420 (1996).
- [14] Mewes, M.-O. *et al.* Collective excitations of a Bose-Einstein condensate in a magnetic trap. *Phys. Rev. Lett.* **77**, 988 (1996).
- [15] Greiner, M., Mandel, O., Esslinger, T., Hänsch, T. W. & Bloch, I. Quantum phase transition from a superfluid to a mott insulator in a gas of ultracold atoms. *Nature (London)* **415**, 39 (2002).
- [16] Mandel, O. *et al.* Controlled collisions for multi-particle entanglement of optically trapped atoms. *Nature (London)* **425**, 937 (2003).
- [17] Calabrese, P. & Cardy, J. Quantum quenches in extended systems. arXiv:0704.1880 (2007); and references therein.
- [18] See the Methods section.
- [19] The constrained theory then gives $\hat{\rho}_c = \exp\left(-\sum_{\alpha=1}^D \lambda_{\alpha} \hat{P}_{\alpha}\right)$, with $\lambda_{\alpha} = -\ln(|C_{\alpha}|^2)$, and D the dimension of the Hilbert space. Notice, however, that in the integrable case in Ref. [10] the number of integrals of motion is equal to the number of lattice sites $N \ll D$.
- [20] Shnirelman, A. I. Ergodic properties of eigenfunctions. *Ups. Mat. Nauk* **29**, 181 (1974).
- [21] Voros, A. *Stochastic Behavior in Classical and Quantum Hamiltonian Systems* (Springer-Verlag, Berlin, 1979).
- [22] de Verdière, Y. C. Ergodicité et fonctions propres du Laplacien. *Commun. Math. Phys.* **102**, 497 (1985).
- [23] Zelditch, S. Uniform distribution of eigenfunctions on compact hyperbolic surfaces. *Duke Math. J.* **55**, 919 (1987).
- [24] Berry, M. V. Regular and irregular semiclassical wavefunctions. *J. Phys. A* **10**, 2083 (1977).
- [25] Korepin, V. E., Bogoliubov, N. M. & Izergin, A. G. *Quantum Inverse Scattering Method and Correlation Functions* (Cambridge University Press, Cambridge, 1993).
- [26] Goldstein, S., Lebowitz, J. L., Tumulka, R. & Zanghì, N. Canonical typicality. *Phys. Rev. Lett.* **96**, 050403 (2006).
- [27] Srednicki, M. Thermal fluctuations in quantized chaotic systems. *J. Phys. A* **29**, L75 (1996).
- [28] We have in fact seen no correlation in the nonintegrable case.
- [29] Srednicki, M. Does quantum chaos explain quantum statistical mechanics? cond-mat/9410046.